NUMERICAL SIMULATION OF WAVE LOADING ON A SPAR PLATFORM

K.M.T. Kleefsman and A.E.P. Veldman
University of Groningen, Department of Mathematics,
P.O. Box 800, 9700 AV Groningen, The Netherlands
E-Mail: theresa@math.rug.nl

SUMMARY

This paper describes a study of simulation of wave loading on a SPAR platform. The method used for the simulations is based on the Navier-Stokes equations, discretised using a finite volume method. The free-surface displacement is described by the VOF-method combined with a local height function. The regular head waves are generated using 5th order Stokes wave theory. To prevent reflections from the walls into the computational domain, a dissipation zone has been used where damping occurs by adding a pressure at the free surface. The results of the validation of regular wave loading on a SPAR platform are found to be very promising.

1 INTRODUCTION

In the offshore industry, floating units are used for the production and storage of oil and gas (FPSOs). These units have to be designed for operation in harsh environments, such as the North Sea or the Gulf of Mexico. When the units are taken into production, they mostly stay at a field for 15 or 20 years, without the possibility of sailing away when a storm is approaching. This means that they must be designed against all weather and wave conditions, and it happened more than once that a unit got into trouble by impacting waves or waves turning over the deck (which is called green water). MARIN initiated the joint-industry project SafeFLOW, which is also sponsored by the European Community, to get more insight in the phenomena playing a role at bow impact and green water at the bow and from the side of a floating offshore unit. Design guidance for floating production units will be developed.

As part of this project, a validated numerical method will be developed for the prediction of local wave impact loads on floaters. The method is implemented in the program ComFLOW. Part of the development and validation of ComFLOW is presented in this study. At the start of the project, the method had been validated for the simulation of pressure loads in case of a dambreak kind of fluid flow over the deck of a ship. The loads on the deck and a deck structure have been calculated and compared to experimental results [2]. With the same method, a coupled solid-liquid dynamics problem from a satellite in space has been simulated [3]. The next step in the development is a study on wave propagation and wave loading. Therefore, waves have been implemented and wave loading experiments have been used to validate ComFLOW. The results of this study will be shown in the present document.

2 MATHEMATICAL MODEL

The fluid flow of an incompressible fluid in a domain V satisfies conservation of mass and momentum. These conservation laws are described by the continuity equation and the Navier-Stokes equations which, in conservative form, are given by

$$\oint_{\partial V} \boldsymbol{u} \cdot \boldsymbol{n} dS = 0, \tag{1}$$

$$\int_V \frac{\partial \boldsymbol{u}}{\partial t} dV + \oint_{\partial V} \boldsymbol{u}\boldsymbol{u}^{\mathrm{T}} \cdot \boldsymbol{n} dS = -\frac{1}{\rho} \oint_{\partial V} (\boldsymbol{p} - \mu \nabla \boldsymbol{u}) \cdot \boldsymbol{n} dS + \int_V \boldsymbol{F} dV. \tag{2}$$

Here, $\boldsymbol{u} = (u, v, w)$ denotes the fluid velocity in the three coordinate directions, $\boldsymbol{n}$ is the normal at the boundary of volume V, ρ denotes density, $\boldsymbol{p}$ is the pressure, and ∇ is the gradient operator. Further μ denotes dynamic viscosity and $\boldsymbol{F} = (F_x, F_y, F_z)$ is an external body force, for example gravity.

On the solid boundaries of the volume and on the objects in the domain, a no-slip condition has been used which is given by $\boldsymbol{u} = 0$. At the free surface, continuity of tangential and normal stresses is demanded. Furthermore, the displacement of the free surface is described by

$$\frac{Ds}{Dt} = \frac{\partial s}{\partial t} + (u \cdot \nabla) s = 0, \tag{3}$$

where $s(\boldsymbol{x}, t) = 0$ gives the position of the free surface.

3 NUMERICAL MODEL

3.1 SOLUTION METHOD

To solve the fluid equations, a fixed Cartesian grid has been used which results in cut-cells where the geometry cuts the grid. The variables have been staggered, which means that the pressure lies in cell

centers, whereas the velocities are placed on the cell faces. Geometry apertures have been introduced to distinguish between solid cells ($F^b = 0$), cells partly open to fluid ($0 < F^b < 1$) and cells completely open to fluid ($F^b = 1$). For the cell faces, similar apertures are used to define which part of the cell faces is open to fluid and which part is not. For the construction of the free surface, a Volume Of Fluid (VOF) function is used which has values $0 \leq F^s \leq F^b$, where $F^s = 0$ means that no fluid is in the cell and $F^s = F^b$ that the cell is completely filled with fluid.

The continuity equation and the Navier-Stokes equations as given in Equation 1 and 2 are discretised in space using a finite volume discretisation. As an example, the discretisation of the continuity equation will be explained in two dimensions. In Figure 1 the control

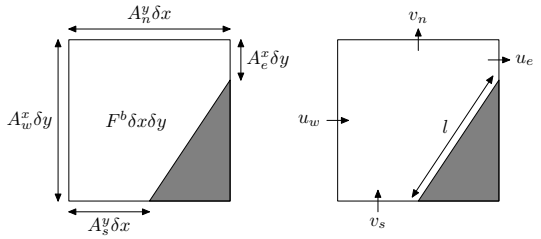

Figure 1: Control volume for the continuity equation

volume of the continuity equation where conservation of mass is demanded has been shown. Conservation of mass in this control volume means that the total flux through its faces equals zero:

$$u_e A_e^x \delta y + v_n A_n^y \delta x - u_w A_w^x \delta y - v_s A_s^y \delta x + 0 \cdot l = 0 \quad (4)$$

Here, A^x, A^y and A^z are the edge apertures in x, y and z direction respectively as shown in the right of Figure 1. The discretisation of the Navier-Stokes equations can be done in the same manner. Details about this discretisation can be found in [3].

The Forward Euler method has been adopted for the time discretisation. After both time and space discretisation has been accomplished, the numerical equations result in

$$M \boldsymbol{u}_h^{n+1} = 0, \quad (5)$$

$$\Omega \frac{\boldsymbol{u}_h^{n+1} - \boldsymbol{u}_h^n}{\delta t} + C(\boldsymbol{u}_h^n)\boldsymbol{u}_h^n = -\frac{1}{\rho}(M^{\mathrm{T}} \boldsymbol{p}_h^{n+1} - \mu D \boldsymbol{u}_h^n) + \boldsymbol{F}_h^n. \quad (6)$$

Here, the time level is denoted by the superscript n, and M, Ω, C and D are coefficient matrices resulting from the spatial discretisation. The continuity equation is discretised on a new time level to ensure that the velocity field is divergence free at that time level.

To solve these equations, the terms of Equation 6 are rearranged such that they can be substituted in Equation 5, which results in a Poisson equation for the pressure. This equation is solved using the Successive Overrelaxation (SOR) method where the optimal relaxation parameter is determined during the iterations [1]. After the pressure field has been solved, the velocities at the new time level can be calculated using the pressure gradient.

The free surface is reconstructed using a piecewise-constant reconstruction technique, after which it is displaced using a donor-acceptor method based on the VOF method developed by Hirt and Nichols [5]. The original method is slightly modified to prevent the flotsam and jetsam the original VOF method suffers from.

3.2 IMPLEMENTATION OF WAVES

For simulation of green water on the deck of a ship or wave impact on the ship's bow, the implementation of waves is necessary. Therefore, an inflow boundary has been placed at the negative x-axis where the wave is coming into the domain, and at the opposite wall some kind of anti-reflection condition has to be implemented.

On the inflow boundary, the wave has been generated by prescribing velocities and wave heights given by an analytical wave description. In the current model, Stokes wave theory has been used which is expanded until 5th order. The implementation has been done according to Skjelbreia [8], where the minus correction in one of the terms has been taken into account.

To prevent waves reflecting into the domain, where they influence the solution, many possible boundary conditions can be used. Givoli [4] gives an overview of the different methods which are being used to prevent wave reflections. Firstly, local non-reflecting boundary conditions are often used, which have the large advantage that there is an outflow boundary directly at the end of the computational domain. This is not the case in the second class, where a dissipation zone has been added at the end of the computational domain which gives a large rise in the number of grid cells. Nevertheless, a variant of this last class has been used in the current method, because it is very general applicable and robust.

For the damping inside the dissipation zone an extra pressure has been added to the free surface as explained in [9] and [7]. Physically, this can be interpreted as the air acting like a damper on the wave. The pressure added to the atmospheric pressure at the free surface is chosen as a function of the vertical velocity at the free surface:

$$p_{damp} = \alpha(x)\, w(x, \eta, t).$$

in which the function $\alpha(x)$ is linear. The most straightforward way of damping is to damp the wave completely. Then, no outflow boundary is needed, because no wave is present at the end of the dissipation

zone. Another possibility is to 'damp' the wave to the analytical wave description, which is then used as boundary condition on the outflow boundary. In [7] also a combination is used of the damping zone which damps the large frequencies and a Sommerfeld condition which is tuned on one (small) frequency. In the study of regular wave loading on a SPAR platform below, damping towards the analytical wave turned out to be most effective.

4 WAVE LOADING ON A SPAR

To validate the program on the issue of wave loading, simulations have been performed of regular wave loading on a SPAR Buoy. At the Maritime Research Institute Netherlands (MARIN), experiments with a SPAR have been performed where the SPAR was fixed while regular waves hit the structure [6]. In full scale, the SPAR has a total length of 220 m and a diameter of 35 m, the draft is 200 m in a water depth of 290.35 m. The SPAR has been divided into three horizontal segments on which forces have been measured (see Figure 2).

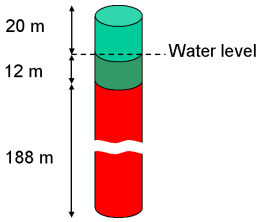

Figure 2: Configuration of the SPAR buoy which is divided into 3 segments

The characteristics of the waves used in the simulations which have been performed are given in the table below.

Test	ω (rad/s)	T (s)	H (M)	λ (m)
101	0.26	24.17	10.77	866
201	0.26	24.17	23.62	866
001	0.48	13.09	10.91	274

The SPAR buoy has been placed at a distance of one wavelength behind the inflow boundary. About 100 m behind the cylinder, a dissipation zone of one wavelength has been added to prevent wave reflections into the domain.

The simulations of wave tests 101 and 102 have been performed on a grid with about 60 cells per wavelength, 15 cells in the transverse direction and 52 cells along the total height of the domain. This amount of grid cells was found to be accurate enough to capture a wave. The grid is stretched in the z-direction towards the calm water level. The wave in these tests is the same, except that the wave height in test 201 is about two times as large. The results of test 101 are shown in Figure 3.

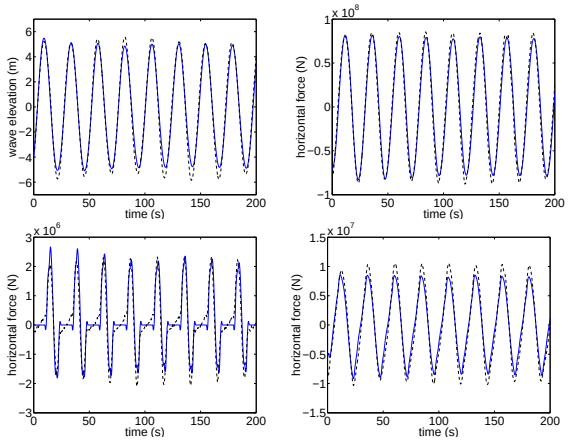

Figure 3: Test 101: top row: wave height 300 m in front of the SPAR (left), total horizontal force on the SPAR (right); bottom row: horizontal force on upper segment (left) and mid segment (right). Solid: ComFLOW, dashed: model test

The global impression of the results is that there is a good agreement between the simulation and the model test. In the upper left of Figure 3 the wave height at about 300 meter in front of the SPAR has been shown. The comparison between the experiment and ComFLOW is satisfying. No phase difference is present and the amplitude of the wave is very much the same except for the trough of the wave which is a bit flatter in the ComFLOW simulation.

In the upper right of Figure 3 the measured horizontal force in the direction of the wave on the center of gravity of the SPAR has been compared to the calculated force and shows a very good agreement. The forces on the upper and mid segments which are shown in the lower part of Figure 3 also show a good agreement. The force on the lower segment is almost equal to the total force on the SPAR and is not shown in this document. The upper segment lies above the calm water level, so this segment comes completely out of the water every period, where the force equals zero. The non-sinusoidal form of the force on the mid segment is also due to the fact that the wetness of the segment is not equal throughout a period.

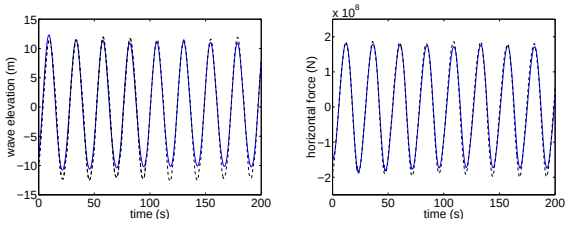

Figure 4: Test 201: wave height 300 m in front of the SPAR (left) and total horizontal force on the SPAR (right). Solid: ComFLOW, dashed: model test

The results of test 201 are much the same as the results presented for test 101. To get a good idea of the

agreement between this model test and the ComFLOW simulation, the wave height 300 meter in front of the SPAR and the total horizontal force in the center of gravity of the SPAR are shown in Figure 4. The wave is really flatter in the troughs, but this does not have a very large influence on the total force on the SPAR.

The third wave loading simulation which has been performed deals with a much shorter (and more realistic) wave. In this case, the influence of the SPAR on the wave is not negligible as it was in the previous cases. This is also shown in the results of the simulation of this wave (with the same number of grid cells per wavelength) of which the pressure at the front of the SPAR and the total horizontal force on the SPAR are shown in Figure 5 (coarse grid). Much more cells are needed around the SPAR, therefore also stretching in x and y direction has been applied in the mid and fine grid of Figure 5. The fine grid has about 3.8 times more grid cells than the coarse grid in the neighbourhood of the SPAR. From Figure 5 it can be concluded that the fine grid does reproduce the model test pretty nicely, whereas the other grids are not accurate enough. In Figure 6 time traces of the horizontal forces on the upper and mid segment of the SPAR have been shown. Both graphs show a rather good agreement with the experiment.

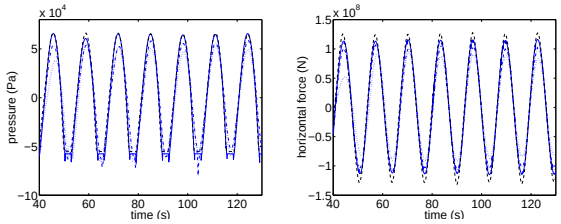

Figure 5: Test 001: Comparison of different grids: wave height at the front of the SPAR (left) and total horizontal force on the SPAR (right). Dotted: ComFLOW coarse grid, dash-dotted: ComFLOW mid grid, solid: ComFLOW fine grid, dashed: model test

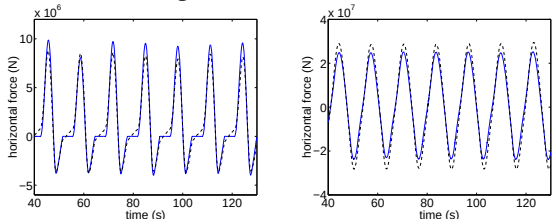

Figure 6: Test 001: Horizontal force on the upper segment (left) and on the mid segment (right) using the fine grid. Solid: ComFLOW, dashed: model test

5 CONCLUSIONS

From the simulations of wave loading on a SPAR platform, it can be concluded that ComFLOW is able to reproduce results from the model tests with a satisfying accuracy. When a long, low wave is hitting the SPAR, the wave is almost not influenced by the SPAR. In that case a rather coarse grid can be used, to reproduce the wave correctly. But when a shorter wave has been used, a much finer grid is necessary to reproduce the details of the flow around the SPAR correctly. The grid choice has shown to be essential in these simulations.

The next step in the development of the method is to implement moving objects, so that wave loading and green water at the bow of a floating unit can be simulated. Also attention will be paid to another way of prescribing the waves. The far wave field and ship motion will be calculated using for example a diffraction code, after which the current method will calculate the details around and at the ship.

6 ACKNOWLEDGEMENTS

The SafeFLOW project is supported by the European Community under the FP5 GROWTH program; the authors are solely responsible for the present paper and it does not represent the opinion of the European Community. It is also supported by 26 parties from the industry (oil companies, shipyards, engineering companies, regulating bodies). MARIN is greatly acknowledged for providing the experimental results of the SPAR platform model tests.

7 REFERENCES

1. Botta, E.F.F., Ellenbroek, M.H.M., *A Modified SOR Method for the Poisson Equation in Unsteady Free-Surface Flow Calculations*, Journal of Computational Physics, **60**, 119-134, 1985.
2. Fekken, G. Veldman, A.E.P., Buchner, B., *Simulation of green-water loading using the Navier-Stokes equations*, J. Piquet, editor, Proceedings 7th International Conference on Numerical Ship Hydrodynamics, 6.3-1-6.3-12, Nantes, 1999.
3. Gerrits, J., *Dynamics of Liquid-Filled Spacecraft - Numerical Simulation of Coupled Solid-Liquid Dynamics*, PhD thesis, University of Groningen, 2001.
4. Givoli, D., *Non-reflecting Boundary Conditions*, Journal of Computational Physics, **94**, 1-29, 1990.
5. Hirt, C.R., Nichols, B.D. *Volume of fluid (VOF) method for the dynamics of free boundaries*, Journal of Computational Physics, **39**, 201-225, 1981.
6. MARIN, *Model Tests on a SPAR Buoy in Waves and Current*, Report No. 15308-1-HT, Maritime Research Institute Netherlands, 2000.
7. Meskers, G., *Realistic Inflow Conditions for Numerical Simulation of Green Water Loading*, Master's Thesis, Delft University of Technology, 2002.
8. Skjelbreia, L., and Hendrickson, J.A., *Fifth Order Gravity Wave Theory*, Proceedings, pp 184-196, 7-th Coastal Engineering Conference, The Hague, 1960.
9. Westhuis, J., *The Numerical Simulation of Nonlinear Waves in a Hydrodynamic Model Test Basin*, PhD thesis, University of Twente, 2001.